

SPARC is a decoy counterpart for c-Fos and is associated with osteoblastic differentiation of bone marrow stromal cells by inhibiting adipogenesis

TOMOYA HATORI^{1,2}, TOYONOBU MAEDA¹, ATSUKO SUZUKI¹,
KEISO TAKAHASHI³ and YASUMASA KATO^{1,2}

¹Department of Oral Physiology and Biochemistry, Ohu University Graduate School of Dentistry;
Departments of ²Oral Function and Molecular Biology, and ³Conservative Dentistry,
Ohu University School of Dentistry, Koriyama, Fukushima 963-8611, Japan

Received April 27, 2022; Accepted November 23, 2022

DOI: 10.3892/mmr.2023.12937

Abstract. Secreted protein acidic and rich in cysteine (SPARC), also called basement-membrane protein 40 or osteonectin, is a matricellular protein that is abundant not only in bone tissue as a non-collagenous protein but is also ubiquitously expressed in non-calcified tissue. SPARC is located intracellularly and disruption of the *Sparc* gene has been reported to reduce bone formation and increase fat tissue; however, the mechanism by which SPARC inhibits adipogenesis remains unclear. The present study evaluated the intracellular function of SPARC in adipogenesis using the bone marrow stromal cell line ST2. When ST2 cells with low SPARC production were cloned, intrinsic activator protein-1 (AP-1) activity was markedly higher, mineralized nodule formation was significantly lower and lipid accumulation was significantly increased compared with in the parental ST2 cells. Forced expression of secreted SPARC with the signal peptide-coding sequences of wild-type *Sparc* or preprotrypsin in SPARC-low ST2 cells significantly reduced AP-1 transcription activity; however, these reductions were not observed in the absence of signal peptide sequences. Recombinant SPARC, produced using *Brevibacillus brevis*, specifically bound to c-Fos but not c-Jun and inhibited the binding of c-Fos/c-Jun to a TPA-response element sequence. These data suggested that SPARC was incorporated into the cells from the extracellular spaces and serves an intracellular role as a decoy counterpart for c-Fos, as well as being associated with osteoblastogenesis through the inhibition of adipogenesis. These findings may provide new insights into regenerative medicine.

Introduction

Secreted protein acidic and rich in cysteine (SPARC), also known as basement-membrane protein 40 or osteonectin, is a 43-kDa glycoprotein classified as a matricellular protein (1,2). SPARC is the most abundant non-collagenous protein in the bone matrix and demonstrates high affinity for calcium, type I collagen and hydroxyapatite, affinities associated with their mineralization (1). Furthermore, SPARC has been reported to localize in non-mineralized tissues, which makes its distribution ubiquitous (3,4). SPARC not only binds to collagen fibrils (types I, II, III and V) but also to basement collagen type IV (5,6) and vascular endothelial growth factor A (7). Phenotypically, mice with *Sparc* gene knock out (KO) are characterized by cataracts, decreases in collagens and bone mineral density, and increases in levels of adipose tissue (8-10). Bone marrow stromal-derived cells from *Sparc* KO mice have been reported to demonstrate reduced ability to form mineralized nodules and reduced osteocalcin (*OCN*) mRNA expression levels, and enhanced adipocyte development through the upregulation of adipisin and CCAAT/enhancer-binding protein δ (*C/EBP δ*) expression levels (11). *Sparc* KO cells have also been reported to show reduced collagen type I and transforming growth factor- β 1 mRNA and protein expression levels (12). Taken together, these findings indicated that SPARC may commit cells to the osteoblast lineage by inhibiting their differentiation into adipocytes.

SPARC has also been reported to localize to nuclei (13,14) and the endoplasmic reticulum (ER) (15). Intracellularly, SPARC has been reported to be associated with tubulin (16) and osteopontin (OPN) (17), and to accumulate in nasopharyngeal angiofibromas (18). Moreover, SPARC was not secreted into the culture medium but was reported to have been detected in lysates of chronic myelogenous leukemia cells (19). Bioinformatics analysis studies have reported that SPARC binds to xeroderma pigmentosum group C complex subunit and zinc finger protein 579 intracellularly (20). Therefore, although SPARC has been reported to be localized intracellularly, its intracellular activity associated with osteoblastogenesis/adipogenesis remains unclear.

Correspondence to: Dr Yasumasa Kato, Department of Oral Function and Molecular Biology, Ohu University School of Dentistry, 31-1 Misumido, Tomita-machi, Koriyama, Fukushima 963-8611, Japan
E-mail: yasumasa_kato@live.jp; y-katou@den.ohu-u.ac.jp

Key words: secreted protein acidic and rich in cysteine, activator protein-1 activity, c-Fos, decoy, adipogenesis, osteoblastogenesis

Adipogenesis by mesenchymal stem cells is induced by several transcription factors, such as peroxisome proliferator-activated receptor- γ (PPAR γ) and C/EBP α . C/EBP β and C/EBP δ are factors that induce PPAR γ - and C/EBP α -expressing preadipocytes, which suggests that PPAR γ and C/EBP α serve roles during the late stages of adipogenic differentiation (21). However, activator protein-1 (AP-1) is an important transcription factor involved in early stage commitment to the adipocyte lineage (21).

AP-1 is a homo- or hetero-dimeric transcription factor consisting of basic region leucine zipper domain proteins, such as Fos and Jun, that translocates into the nucleus. Although the Fos proteins, such as c-Fos, Fra-1, Fra-2, FosB and the short isoform of FosB (Δ FosB), heterodimerize only with their counterpart Jun proteins, such as c-Jun, JunB and JunD, the Jun proteins homodimerize or heterodimerize with Fos proteins. The Fos/Jun and Jun/Jun dimers bind to TPA-response element (TRE; 5'-TGACTCA-3') (22). c-Fos has been reported to induce the production of adipocyte P2/fatty acid-binding protein 4 (FABP4), which serves an important role in adipogenesis (23). Mutations in the *c-FOS* gene have been reported to predict the phenotypic development of congenital generalized lipodystrophy and Berardinelli-Seip congenital lipodystrophy, rare genetic syndromes characterized by the absence of adipose tissue (24), which suggests that c-Fos is important for adipogenesis. The present study evaluated whether SPARC interacted with c-Fos to commit to the osteoblastic lineage by the inhibition of adipogenesis.

Materials and methods

Reagents. RPMI 1640 medium and simvastatin were purchased from MilliporeSigma; α -minimum essential medium (α -MEM) was purchased from MP Biomedicals; and ascorbic acid, β -glycerophosphate alizarin red-S, Oil red O and ethidium bromide were purchased from FUJIFILM Wako Pure Chemical Corporation. Fetal bovine serum (FBS) was purchased from Hyclone (Cytiva). Guanidinium thiocyanate, phenol, chloroform and Bacto Yeast Extract were purchased from Nacalai Tesque, Inc. Prime STAR GXL DNA Polymerase and Xfect Transfection Reagent, SYBR Premix Ex *Taq* II, In-Fusion[®] HD Cloning Kit and *Brevibacillus* expression system II were purchased from Takara Bio, Inc.; and Blocking Regent N102 was from NOF Corporation. Immobilon-P polyvinylidene fluoride (PVDF) membranes and the chemiluminescent reagent Luminata[™] Forte Western HRP substrate were purchased from MilliporeSigma; and Hybond-C nitrocellulose membranes and Hybond-N+ nylon membranes were purchased from GE Healthcare. Radioimmunoprecipitation assay (RIPA) Buffer, Dulbecco's modified Eagle medium (DMEM), Bacto[™] Soytone, SuperScript IV Reverse Transcriptase and a High-Capacity cDNA Reverse Transcription Kit (cat. no. 4387406) were purchased from Thermo Fisher Scientific, Inc. Prime STAR GXL DNA Polymerase and Dual-Luciferase[®] Reporter Assay System were purchased from Promega Corporation; and avidin-linked HRP and DC^o protein assay kits were from Bio-Rad Laboratories, Inc.

Antibodies. Anti-SPARC polyclonal antibody (pAb) (1:1,000; cat. no. ab55847) was purchased from Abcam, anti-c-Jun (G-4) monoclonal antibody (mAb) (1:1,000; cat. no. sc-74543), and anti-c-Fos (H-125) mAb (1:1,000; cat. no. sc-7202) were purchased from Santa Cruz Biotechnology, Inc. Anti- β actin pAb (1:1,000; cat. no. GTX109639) and anti-GAPDH pAb (1:1,000; cat. no. GTX100118) were purchased from GeneTex, Inc.; anti-Lamin-A pAb (1:1,000; cat. no. 3267) was purchased from BioVision, Inc. Anti-FLAG M2 mAb (1:1,000; cat. no. F1804) was purchased from MilliporeSigma; and biotin-conjugated anti-rabbit IgG pAb (1:10,000; cat. no. 111-065-144) and biotin-conjugated anti-mouse IgG pAb (1:10,000; cat. no. 115-065-003) were purchased from Jackson ImmunoResearch Laboratories.

Vectors. p3xFLAG-CMV-9 and p3xFLAG-CMV-10 vectors were purchased from MilliporeSigma. The pAP1(1)-Luc vector was purchased from Affymetrix, Inc.; pGL4.75[hRluc CMV] was from Promega Corporation; and pNCMO2 was from Takara Bio, Inc.

Sequence datasets. Sequence data for cDNA and proteins were downloaded from the National Center for Biotechnology Information (<https://www.ncbi.nlm.nih.gov>). Accession numbers for the datasets used were as follows: Human SPARC (NM_003118.4 and NP_003109.1); mouse SPARC (NM_009242.5); mouse c-Fos, cDNA (NM_010234.2 and NP_034364); mouse c-Jun (NM_010591.2 and NP_034721.1).

Cells and cell culture. The mouse bone marrow stromal ST2 cell line was purchased from the RIKEN BioResource Center (25,26). The human oral cancer Ca9-22 cell line was a gift from Dr Kimiharu Hirose (Ohu University School of Dentistry, Koriyama, Japan) and was originally obtained from Japanese Collection of Research Bioresources Cell Bank (27). ST2 cells were cultured in RPMI 1640 supplemented with 10% FBS and used for osteoblastic and adipocyte differentiation experiments (28). Ca9-22 cells were cultured in DMEM supplemented with 10% FBS and used for cloning of the *SPARC* gene. All cultures were maintained at 37°C under a humidified atmosphere containing 5% CO₂ (unless otherwise noted).

The ST2 cell clone with low SPARC production (Fig. 1A) was selected using the limiting dilution method. Briefly, ST2 cells were inoculated into a 96-well culture plate at a density of 1 cell/well in RPMI 1640 supplemented with 10% FBS; this culture medium was used throughout cell cloning. Immediately after inoculation, an inverted phase-contrast microscope was used to demonstrate that there was 1 cell/well. When the colony formed 2 weeks after seeding, cell culture vessels were scaled up stepwise when they reached 70-80% confluence after culturing for ~10 days: i.e., one well of a 96-well plate, one well of a 24-well culture plate, one well of a 6-well plate, and three wells of a 6-well plate. When cells reached 70-80% confluence in three wells in a 6-well plate, with cells in one well used for RNA extraction, those in the other used for cell lysate preparation and those remaining frozen at -80°C as the stock. SPARC mRNA and protein expression levels were assessed using reverse transcription-quantitative PCR (RT-qPCR) and western blotting, respectively. Finally, the clone where SPARC

Table I. Sequences of primers used for reverse transcription-PCR.

Gene	Sequence, 5'-3'	Product, bp	Accession number
<i>Sparc</i>	F: ATGAGGGCCTGGATCTTCTTTCTCCTTT R: TTAGATCACCAGATCCTTGTTGATGTCCTG	909	NM_001290817.1
<i>Actb</i>	F: CGCAGCCACTGTCGAGTC R: AAGGTCTCAAACATGATCTGGGT	467	NM_007393.5
<i>SPARC</i>	F: ATGAGGGCCTGGATCTTCTTTCTCCTTT R: GATCACAAGATCCTTGTCGATATCCTTCTG	909	NM_003118.4
<i>c-Fos</i>	F: ATGATGTTCTCGGGTTTCAACGCCGACTAC R: TTCTCTGACTGCTCACAGGGCCAGCA	1,155	NM_010234.2
<i>c-Jun</i>	F: ATGACTGCAAAGATGGAAACGACCTTCTAC R: TCAAAACGTTTGCAACTGCTGCGTTAG	1,005	NM_010591.2

F, forward, R, reverse; SPARC, secreted protein acidic and rich in cysteine.

mRNA was not detected after 30 cycles of RT-qPCR was used for subsequent experiments in the present study, these cells were subsequently referred to as SPARC-low ST2 cells.

For osteoblastic differentiation, 70% confluent ST2 cells were incubated with α -MEM supplemented with 10% FBS, 50 μ g/ml ascorbic acid and 10 mM β -glycerophosphate for 3 weeks. In some cases, 10⁻⁶ M simvastatin was also added and cultured for 3 weeks. Calcified deposits were assessed by staining with 40 mM alizarin red-S (pH, 4.2) at room temperature for 10 min. After washing with distilled water five times, images of the culture plates were captured using a digital camera and the red-stained areas were quantified using ImageJ software version 1.5.3 (National Institutes of Health) (26). For adipocyte differentiation, 70% confluent ST2 cells were further incubated with RPMI 1640 medium supplemented with 5 mg/ml insulin, 1 mM dexamethasone and 0.5 mM 1-methyl-3-isobutylxanthine (IBMX) for 2 weeks. Triacylglycerol (TAG) deposits were assessed by staining with Oil Red O at room temperature for 10 min. After washing with 60% isopropanol three times, Oil Red O-stained images of culture plates were captured using a digital camera and high-power images were also captured by an inverted light microscope (objective magnification, x20), and Oil Red O was eluted using 100% dimethyl sulfoxide at room temperature for 5 min and quantified using spectrophotometry at 531 nm (25).

Construction of expression vectors for SPARC and its mutant and transfection. Total RNA was extracted from Ca9-22 cells using the standard acid guanidinium-phenol-chloroform (AGPC) extraction method (29). RNA was reverse transcribed using SuperScript IV Reverse Transcriptase at 55°C for 10 min followed by 80°C for 10 min for inactivation of the enzyme and cDNA was amplified using Prime STAR GXL DNA Polymerase and specific primers (Table I). The qPCR thermocycling protocol consisted of denaturation at 98°C for 10 sec, followed by 30 cycles of annealing at 60°C for 15 sec and extension at 68°C for 60 sec. The resulting fragments were cloned into the vectors p3xFLAG-CMV-9 and p3xFLAG-CMV-10. The amino acid sequence of human SPARC (Fig. 2B) consisted of amino acid residues (AA) 1-17 as the signal peptide and AA 18-303 as the mature protein. The expression vectors were

constructed using the In-Fusion[®] HD Cloning Kit as follows: SPARC (AA 18-303) with wild-type signal peptide (AA 1-17), SPARC (AA 18-303) with preprotrypsin signal peptide, and SPARC (AA 18-303) without signal peptide (Fig. 2C). To confirm the existence of the ectopically expressed SPARC in the conditioned medium (CM), a SPARC-expression vector in which the FLAG sequence was inserted between wild-type signal peptide (AA 1-17) and mature SPARC (AA 18-303) was also generated.

Transfection of vectors into SPARC-low ST2 cells was proceeded using Xfect Transfection Reagent according to the manufacturers' protocol. Briefly, 5 μ g plasmids were mixed with 1.5 μ l Xfect polymer and incubated at room temperature for 10 min, followed by the mixture being added to the cultures in a 6-well culture plate. After incubation of the cells in a CO₂ incubator for 4 h, the culture medium was refreshed and the cells were further incubated for 24 h for AP-1 measurements and 48 h for preparation of CM.

Preparation of SPARC-present/absent CM. SPARC-low ST2 cells were transfected with mock or Flag-tagged SPARC expression vector as aforementioned. Post-transfection, the medium was refreshed with RPMI 1640 supplemented with 10% FBS, and the cells were incubated for a further 48 h. The CM was collected and clarified by centrifugation at 1,000 x g for 10 min to obtain the following: SPARC (+) CM and SPARC (-) CM.

Serum-free SPARC (+) or (-) CM was prepared from the parallel cultures and subjected to western blot analysis. Briefly, after the transfected cells were cultured for 24 h in RPMI 1640 supplemented with 10% FBS, they were cultured for a further 24 h in serum-free RPMI 1640. The serum-free CM was collected and clarified by centrifugation at 1,000 x g at room temperature for 10 min. The supernatant was analyzed by western blotting.

RT-PCR and RT-qPCR. Total RNA was extracted from parental ST2 cells, SPARC-low ST2 cells and transfected cells using the (AGPC) extraction method. RNA was reverse transcribed at 55°C for 10 min, followed by 80°C for 10 min for inactivation of the enzyme, using SuperScript IV Reverse

Table II. Sequences of primers used for reverse transcription-quantitative PCR.

Genes	Sequence, 5'-3'	Accession number
<i>Tgfb2</i>	F: AGTTTACACTGCCCCTGCT R: AGAGGTGCCATCAATACCTGC	NM_009367.4
<i>Alp1</i>	F: GCAGTATGAATTGAATCGGAACAA R: ATGGCCTGGTCCATCTCCAC	NM_007431.3
<i>Col1a1</i>	F: GACATGTTTACGCTTTGTGGACCTC R: GGGACCCTTAGGCCATTGTGTA	NM_007742.4
<i>Bglap</i>	F: CAACAGGAGGGTGCAGAACAGA R: GCTTGGACATGAAGGCTTTGTC	NM_001305448.1
<i>Cfd</i>	F: GGATGGAGTGACGGATGACG R: TGAGGCACTACACTCTGCAC	NM_013459.4
<i>Fabp4</i>	F: TGAAATCACCGCAGACGACA R: ACACATTCCACCACCAGCTT	NM_024406.4
<i>Pparg2</i>	F: GCTTATTTATGATAGGTGTGATC R: GCATTGTGAGACATCCCCAC	NM_001127330.2
<i>Slc2a4</i>	F: GCCCGGACCCTATACCCTAT R: GGGTTCCCCATCGTCAGAG	NM_009204.2
<i>Actb</i>	F: CATCCGTAAAGACCTCTATGCCAAC R: ATGGAGCCACCGATCCACA	NM_007393.5

F, forward, R, reverse; *Tgfb2*, transforming growth factor β 2; *Alp1*, alkaline phosphatase; *Col1a1*, type I collagen; *Bglap3*, osteocalcin; *Cfd*, adipisin; *Fabp4*, fatty acid-binding protein 4; *Pparg2*, proliferator-activated receptor- γ 2; *Slc2a4*, glucose transporter type 4.

Transcriptase with Oligo dT for PCR and at 37°C for 60 min, followed by 95°C for 5 min for inactivation of the enzyme, using a High-Capacity cDNA Reverse Transcription Kit for qPCR.

For RT-PCR, the resultant cDNA was amplified using Prime STAR GXL DNA Polymerase using specific primers (Table I). The thermocycling protocol consisted of 98°C for 30 sec, followed by 30 cycles for *Sparc* or 19 cycles for *Actb* of denaturation at 98°C for 10 sec, annealing at 60°C for 15 sec and extension at 68°C for 60 sec. The PCR products were separated using 1% agarose gel electrophoresis with 10 mM sodium borate medium and visualized using 0.5 μ g/ml ethidium bromide staining at room temperature for 20 min.

For quantification of mRNA expression, the resultant cDNA was amplified using SYBR Premix Ex *Taq* II in a TP-870 Thermal Cycler Dice Real Time System (Takara Bio, Inc.) with specific primers (Table II). Two-step thermal cycling after an initial denaturation phase at 95°C for 30 sec was used in the present study as follows: 45 cycles of denaturation at 95°C for 5 sec and, annealing and extension at 60°C for 30 sec. The mRNA expression levels of each target gene were normalized relative to the mRNA expression levels of *Actb* in the same samples. The data were assessed using the $2^{-\Delta\Delta C_q}$ method (30).

AP-1 activity. AP-1 activity was assessed using a luciferase reporter assay. Briefly, SPARC-low ST2 cells were seeded at a density of 1×10^5 cells/well in 24-well culture plates, incubated overnight in a CO₂ incubator and co-transfected at 37°C for 4 h with the AP1(1) Luc vector and the pGL4.75 vector using Xfect Transfection Reagent. After removal of the transfection reagent, the cells were incubated for an additional 24 h at 37°C

and luminescence intensity was assessed using a TriStar2 LB942 plate reader (Titertek-Berthold) using a dual reporter assay kit (31). The data was normalized to co-transfected *Renilla* luciferase activity.

Western blotting. Whole cell lysates of parental ST2 cells, SPARC-low ST2 cells and transfected cells were prepared using RIPA buffer. Nuclear fractions were extracted as described previously (32). Briefly, 1×10^6 cells were lysed using 400 μ l Buffer A [10 mM HEPES-NaOH, pH 7.9; 10 mM KCl; 0.1 mM EDTA; 1 mM DTT and 0.5 mM phenylmethylsulfonyl fluoride (PMSF)] and incubated on ice for 20 min. The suspensions were centrifuged at 21,000 x g for 10 sec, and the supernatants were collected as post-nuclear fractions. The precipitates were resuspended in 50 μ l Buffer C [20 mM HEPES-NaOH, pH 7.9; 100 mM KCl; 1 mM MgCl₂; 0.2 mM CaCl₂; 0.2 mM EDTA; 10% (v/v) glycerol; 1 mM DTT and 0.2 mM PMSF] and incubated on ice for 20 min, followed by centrifugation of the suspensions at 21,000 x g for 2 min, with the resultant supernatants collected as nuclear extracts. Following reduction with DTT, 10 μ g protein aliquots were separated by SDS-PAGE on 10% gels, followed by transfer of the proteins to PVDF membranes. The membranes were blocked by incubation with TBS-T (20 mM Tris-HCl, pH 7.5; 150 mM NaCl; 0.05% Tween-20) containing 20% blocking reagent N102 at room temperature for 1 h, followed by overnight incubation with the aforementioned primary antibodies at 4°C overnight and incubation with the aforementioned biotinylated secondary antibodies for 1 h at room temperature. The blots were subsequently incubated with streptavidin-conjugated HRP for 20 min at room temperature, and the signals were

detected using Luminata™ Forte Western HRP luminescent substrate (33).

Preparation of recombinant proteins using *Brevibacillus brevis*. Total RNA, which was extracted from Ca9-22 cells for *SPARC* and parental ST2 cells for *c-Fos* and *c-Jun*, according to the AGPC extraction method, was reverse transcribed at 55°C for 10 min using SuperScript IV Reverse Transcriptase with Oligo dT. cDNA was amplified using the Prime STAR GXL DNA Polymerase kit, as follows: Initial denaturation at 98°C for 30 sec, followed by 30 cycles of denaturation at 98°C for 10 sec, annealing at 60°C for 15 sec and extension at 68°C for 3.5 min (*SPARC*) or 60 sec (*c-Fos* and *c-Jun*). The specific primers are shown in Table I. The resultant cDNAs were cloned into the vector pNCMO2 with 4xHis sequences using an In-Fusion® HD Cloning Kit according to the manufacturer's protocol. The details of the cloned genes were as follows: *SPARC* [human, NM_003118.4 (nt 116-973 corresponding to AA 18 to 303)]; *c-Fos* [mouse, NM_010234.2 (nt 140-1282 corresponding to AA 1 to 330)]; *c-Jun* [mouse, NM_010591.2 (nt 952-1956 corresponding to AA 1 to 334)]. These constructs were transfected into *Brevibacillus brevis* using the *Brevibacillus* expression system II. Each protein-expressing strain was cultured in 2SY medium (20.0 g/l glucose, 40.0 g/l Bacto Soytone, 5.0 g/l Bacto Yeast Extract, 0.15 g/l CaCl₂·2H₂O) at 37°C overnight and the culture supernatants were subjected to Ni Sepharose excel (cat. no. 17-3712-01; GE Healthcare) chromatography to purify these proteins according to the manufacturer's protocol.

Electrophoretic mobility shift assay (EMSA). EMSA was performed using oligo DNA with a biotinylated 5'-end. Briefly, the following sequences: DNA oligonucleotide containing TRE sequence forward (F), 5'-TGA GTC AAT GAG TCA GCT GAC TCA TTG ACT CA-3' and reverse (R), 5'-GGT GAG TCA ATG AGT CAG CTG ACT CAT TGA CTC A-3'; and DNA oligonucleotide containing mutant TRE sequence F, 5'-TGT GAC AAT GTG ACA GCT GTC ACA TTG TCA CA-3' and R, 5'-GGT GTG ACA ATG TGA CAG CTG TCA CAT TGT CAC A-3', were annealed and used as probes (underlined bases indicate mutation positions of the TRE element). Recombinant proteins (2 µg), which were prepared using the *Brevibacillus* expression system II as aforementioned, were incubated with probes (2 fmol) in buffer containing 10 mM Tris (pH 7.5), 50 mM KCl, 5 mM MgCl₂, 1 mM DTT, 100 ng Poly(dI/dC), 4% glycerol and 0.05% NP-40 for 15 min at room temperature, followed by electrophoresis on undenatured 4% PAGE. The nucleic acids were subsequently transferred to Hybond-N+ membranes and detected using avidin-conjugated HRP and HRP luminescent substrate (34).

Far western blotting. To evaluate the direct binding of *SPARC* and AP-1 components, far western blotting was performed using recombinant proteins: The subjected protein is blotted on the membrane and then the candidate protein of the counterpart is overlaid. Finally, the yielded complex on the membrane is detected. This assay is considered suitable to assess the direct binding of proteins and is comparable with other assays, such as the immunoprecipitation assay, which are also able to detect indirect binding complex. Briefly, recombinant proteins (0.5, 1.0 and 2.0 µg) from *Brevibacillus brevis* were spotted onto

Hybond-C membranes. Membranes were blocked using 5% skim milk at room temperature for 1 h, then 1.2 µg/cm² of each recombinant protein (*c-Fos*, *c-Jun* and *SPARC*) was overlaid and incubated at room temperature for 1 h. They were blocked again using 10% N102 blocking solution in TBST. After washing with TBST, the primary antibodies (anti-*SPARC*, anti-*c-Fos* and anti-*c-Jun*) were used to detect their respective proteins, according to the aforementioned method described for western blotting.

Protein assay. Protein concentrations were determined prior to western blotting, EMSA and far western blotting according to the Lowry protein assay method using DC™ protein assay kits with bovine serum albumin as the standard, according to the manufacturer's protocol.

Statistical analysis. All experiments were performed in triplicate to ensure that ≥2 independent experiments yielded similar results. Results were presented as the mean ± standard error of the mean (n=3). Comparisons between two independent groups were evaluated using unpaired Student's t-test using Microsoft Excel version 2210 (Microsoft Corporation) and multiple comparisons of ≥3 groups were evaluated using one-way ANOVA followed by Scheffé's F-test (https://astatsa.com/OneWay_Anova_with_TukeyHSD/). P<0.05 was considered to indicate a statistically significant difference.

Results

Phenotype of *SPARC*-low ST2 cells. A clone without obvious expression of *SPARC* was selected from parental ST2 cells and was thereafter named *SPARC*-low ST2 cells. The mRNA and protein expression levels of *SPARC* in the parental and *SPARC*-low ST2 cells were shown in Fig. 1A. *SPARC*-low ST2 cells did not express *Sparc* mRNA nor secrete *SPARC* into the culture medium, although a non-specific signal showing the almost same molecular weight as *SPARC* was detected from the lysate (Fig. 1A). Culture of these *SPARC*-low ST2 cells in osteogenic differentiation medium containing ascorbic acid and β-glycerophosphate reduced calcification when compared with parental ST2 cells (Fig. 1B), which is in agreement with previous reports (11,35). Simvastatin has been reported to be a strong promoter of calcification in the presence of ascorbic acid and β-glycerophosphate (36), an effect which was significantly lower in *SPARC*-low ST2 cells than in the parental cell line (Fig. 1B). RT-qPCR demonstrated that the mRNA expression levels of osteoblastic differentiation-associated genes, such as alkaline phosphatase, transforming growth factor β2 and type I collagen were significantly lower in *SPARC*-low ST2 cells compared with those in parental ST2 cells. However, *Runx2* and osteocalcin mRNA expression levels were not significantly altered in *SPARC*-low ST2 cells compared with those in parental ST2 cells (Fig. 1C). Whether there were changes in the rate of adipogenic differentiation in *SPARC*-low ST2 cells was then assessed using adipogenic differentiation medium containing insulin, IBMX and dexamethasone. This medium induced TAG deposition in parental ST2 cells; however, accumulation was significantly higher in *SPARC*-low ST2 cells compared with that in parental ST2 cells (Fig. 1D). The mRNA expression levels of adipogenesis-related genes,

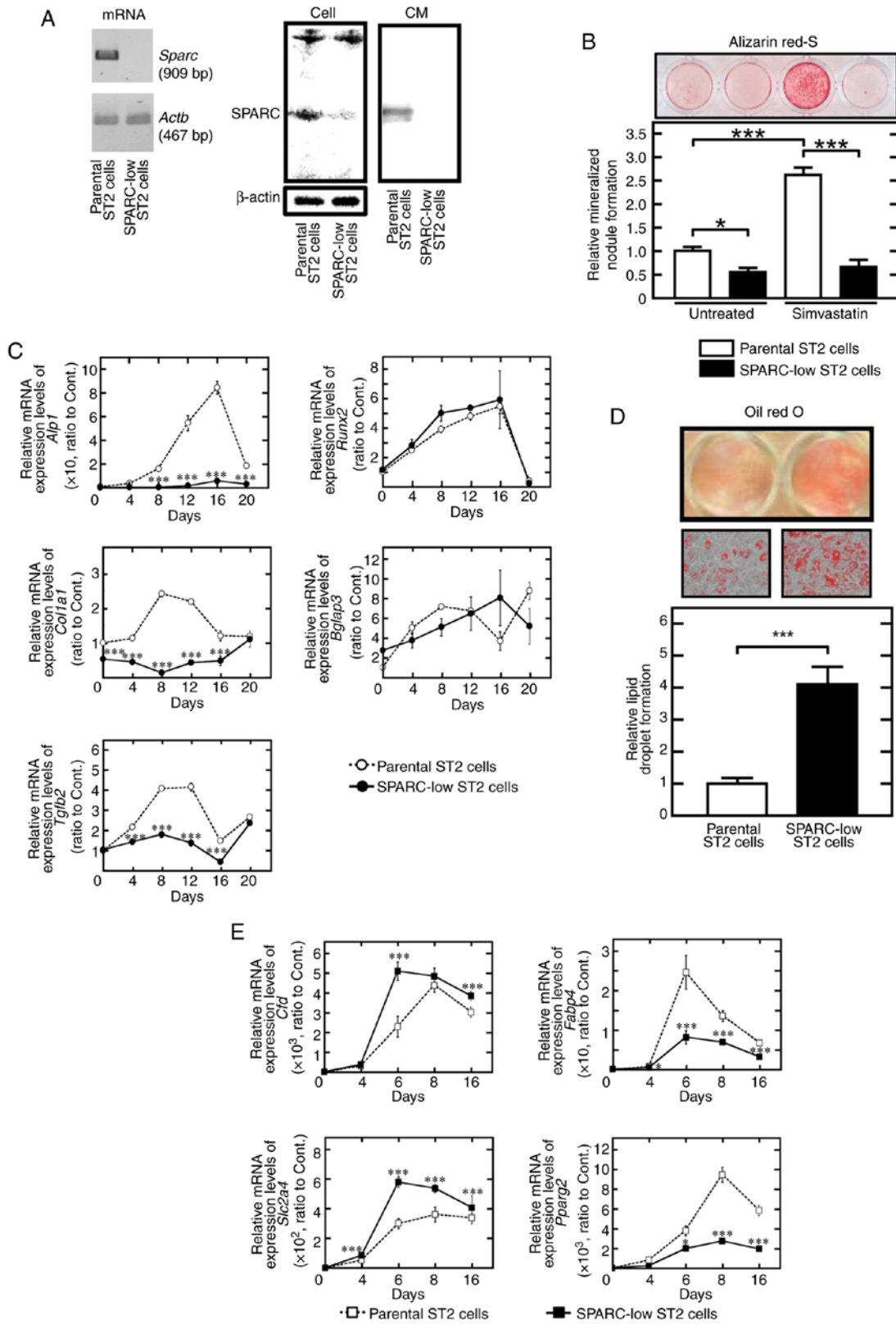


Figure 1. Adipogenesis is higher but osteoblastogenesis is lower in SPARC-low ST2 cells compared with in parental ST2 cells. (A) SPARC expression was assessed at the mRNA and protein levels in cells and CM using RT-PCR and western blotting. (B) SPARC-low ST2 cells demonstrated low mineralized nodule formation activity. Data were presented relative to those of parental ST2 cells cultured in osteogenic medium without simvastatin. (C) Relative mRNA expression levels of osteoblastogenesis-associated genes, including *Runx2*, *Tgfb2*, *Alpl*, *Colla1* and *Bglap3* were assessed using RT-qPCR. The mRNA expression levels were normalized against each control, which was non-stimulated (time 0) parental ST2 cells. (D) SPARC-low ST2 cells demonstrated significantly higher lipid droplet formation activity compared with parental ST2 cells. (High-power images, objective magnification, $\times 20$). The data were presented relative to those of parental ST2 cells cultured in adipogenic medium. (E) Relative mRNA expression levels of adipogenesis-associated genes, including *Cfd*, *Fabp4*, *Pparg2* and *Slc2a4* were assessed using RT-qPCR. The mRNA expression levels were normalized against each control which was non-stimulated (time 0) parental ST2 cells. * $P < 0.05$ and *** $P < 0.001$. CM, conditioned medium; RT, reverse transcription; qPCR, quantitative PCR; Sparc/SPARC, secreted protein acidic and rich in cysteine; *Alpl*, alkaline phosphatase; *Colla1*, type I collagen; *Bglap3*, osteocalcin; *Cfd*, adipisin; *Fabp4*, fatty acid-binding protein 4; *Pparg2*, proliferator-activated receptor- γ ; *Slc2a4*, glucose transporter type 4; *Tgfb2*, transforming growth factor $\beta 2$.

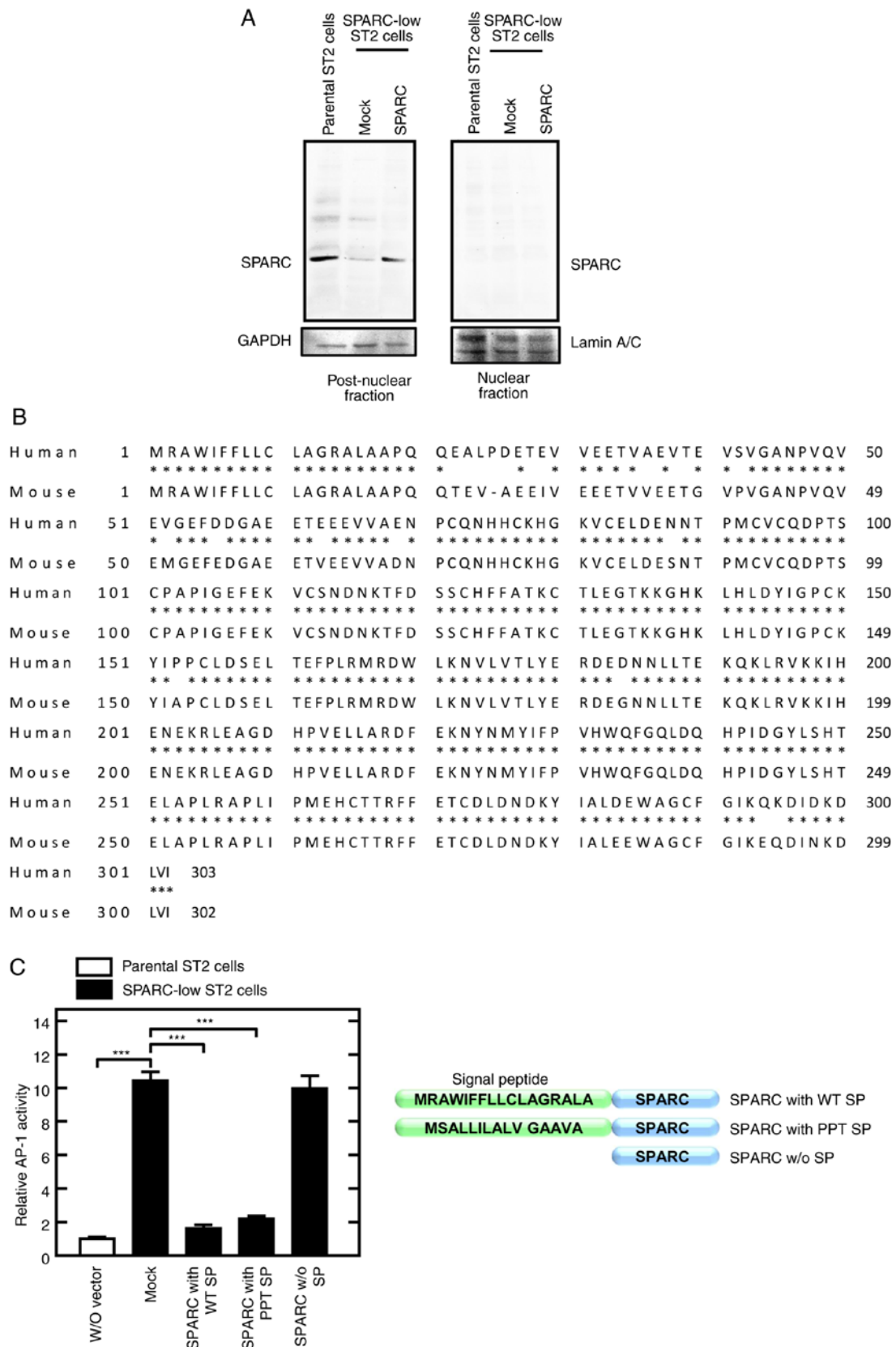


Figure 2. Rescued secreted SPARC localizes to the post-nuclear fraction and inhibits AP-1 activity. (A) SPARC localized to the post-nuclear fraction. Cells were lysed and fractionated into nuclear and post-nuclear fractions. SPARC protein expression levels were assessed using western blotting. Lamin A/C and GAPDH were used as internal controls for the nuclear fraction and post-nuclear fraction, respectively. Mock, empty vector. (B) Comparison of the amino acid sequences of human and mouse SPARC. The amino acid sequences of SPARC were downloaded from NCBI (human, NP_003109.1; mouse, NP_033268.1). Mouse SPARC was 92% homologous with human SPARC including the signal peptide (AA 1 to 17). (C) Secreted SPARC reduced AP-1 activity (left panel). Cells were transfected with the AP1(I)-Luc vector, with or without SPARC expression vectors, as follows: w/o vector; Mock, empty vector; SPARC (AA 18 to 303) with WT SP; SPARC (AA 18 to 303) with PPT SP (AA 1 to 17); SPARC (AA 18 to 303) w/o SP. Luciferase activity was measured 24 h after transfection. N-terminal structure of the SPARC expression vectors is illustrated (right panel). *** $P < 0.001$. AP-1, activator protein-1; AA, amino acid residue; SPARC, secreted protein acidic and rich in cysteine; w/o, without; WT, wild type; SP, signal peptide; PPT, preprotrypsin.

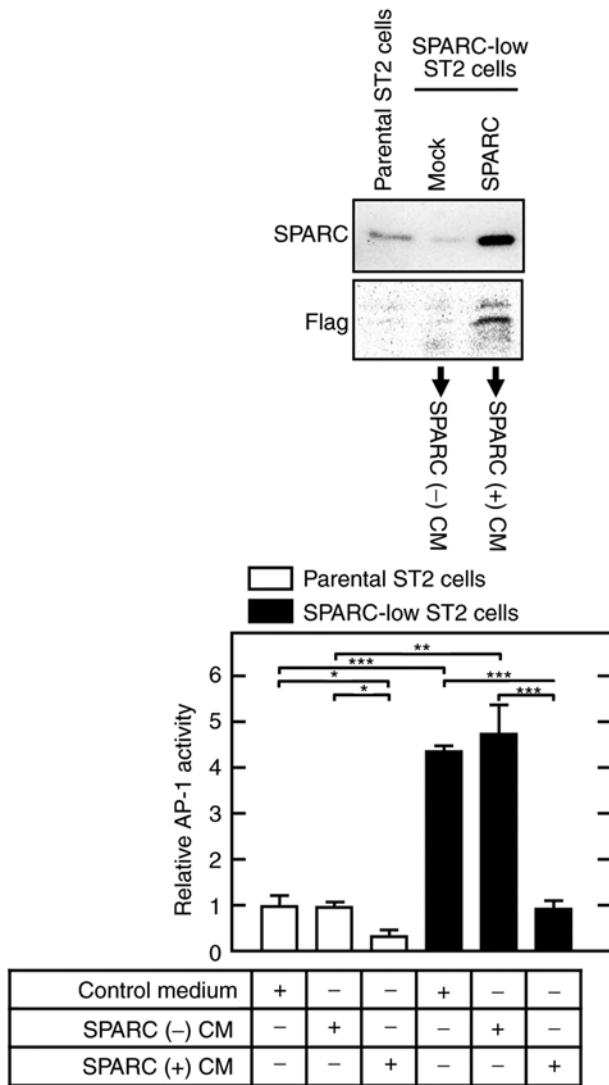


Figure 3. Secreted SPARC reduces AP-1 activity. CM from SPARC-low ST2 cells that had been transfected with SPARC expression vector with wild-type signal peptide, which had a FLAG sequence inserted between the signal peptide (AA 1 to 17) and mature protein (AA 18 to 303), or with the mock vector were obtained [SPARC (+) CM or SPARC (-) CM]. Cells were transfected with AP1(1) Luc vector and treated using SPARC (+) CM or SPARC (-) CM, followed by evaluation of AP-1 activity using the luciferase reporter assay. * $P < 0.05$, ** $P < 0.01$ and *** $P < 0.001$. AP-1, activator protein-1; SPARC, secreted protein acidic and rich in cysteine; CM, conditioned media.

such as adipsin and glucose transporter 4 were significantly higher in SPARC-low ST2 cells compared with those in the parental ST2 cells. In addition, the mRNA expression levels of *Pparg2* and *Fabp4* were induced by adipogenic differentiation medium; however, the induced mRNA expression levels were, unexpectedly, significantly lower in SPARC-low ST2 cells compared with those in parental ST2 cells (Fig. 1E). *Fabp4* KO preadipocytes have previously been reported to differentiate to adipogenic cells more than *Fabp4* WT cells (37), which suggested that the contribution of FABP4 to adipogenesis was dependent on the differentiation state of the cells (preadipocytes vs. bone marrow stromal cells). Phenotypically, SPARC-low ST2 cells resemble the cells derived from *Sparc* KO mice (8-10). The 3T3-L1 cell line has been used for adipogenic differentiation or as an adipocyte

model (38); however, it has not been reported to differentiate into osteoblasts. The MC3T3-E1 cell line has been used to assess osteoblastic differentiation (26), but has rarely been reported to differentiate into adipogenic cells. However, ST2 cells have the phenotypic ability to differentiate into either cell type depending on the culturing conditions. These findings indicated that ST2 cells were a more appropriate model to test the effects of SPARC than 3T3-L1 and MC3T3-E1 cells.

Extracellular SPARC incorporated into cells reduces AP-1 activity. The intracellular function of SPARC was initially evaluated by assessing its presence in the nuclear and post-nuclear fractions of ST2 cell lysates, and in their CM. SPARC was not detected in the nucleus but was demonstrated in the post-nuclear fractions of both parental ST2 cells and SPARC-rescued SPARC-low ST2 cells (Fig. 2A) and their CM (Fig. 3). The amino acid sequence of human SPARC is highly conserved among animal species (92% homology with mouse origin) (Fig. 2B); therefore, the SPARC expression vector was constructed using human cDNA.

The effects of *Sparc* expression on AP-1 activity were evaluated using the TRE-driven luciferase expression vector. AP-1 activity was significantly higher in SPARC-low ST2 cells compared with its activity in parental ST2 cells. However, the induction of SPARC expression using a signal peptide derived from SPARC or preprotrypsin significantly reduced the activity levels of AP-1 in SPARC-low ST2 cells compared with in the SPARC-low ST2 cells (Fig. 2C); however, this reduction was not demonstrated when SPARC was expressed without the signal peptide. These data suggested that the intracellular localization of SPARC depended on its signal peptide sequence. Although it was initially hypothesized that the intracellular localization of SPARC was due to the SPARC WT signal peptide, the effect of replacement of the SPARC WT signal peptide with preprotrypsin signal peptide was not significant and SPARC lacking signal peptide demonstrated no AP-1 inhibitory activity, which suggested that AP-1 inhibition occurred due to incorporation of the secreted SPARC rather than intracellularly expressed SPARC.

When SPARC-low ST2 cells and their parental cells were cultured in CM from SPARC-rescued SPARC-low ST2 cells [SPARC (+) CM], AP-1 activity was significantly lower compared with that in cells cultured in CM from mock-transfected SPARC-low ST2 cells [SPARC (-) CM] (Fig. 3). Furthermore, the increased AP-1 activity in SPARC-low ST2 cells was markedly reduced by SPARC (+) CM treatment to a similar level to that shown in control/SPARC (-) CM-treated parental ST2 cells. These results suggested that SPARC was secreted into the extracellular space and incorporated into the cytosol, where it interfered with the AP-1 complex/consensus sequence.

SPARC binds c-Fos. To evaluate whether SPARC reduced AP-1 transcription activity by interfering with its dimerization, the recombinant peptides c-Fos, c-Jun and SPARC were expressed in *Brevibacillus brevis*, and EMSA was performed using these peptides and a double-strand oligonucleotide containing the TRE sequence or non-consensus sequence (mutant TRE) as the negative control (Fig. 4). The complex electrophoretically migrated slower than the free DNA oligo

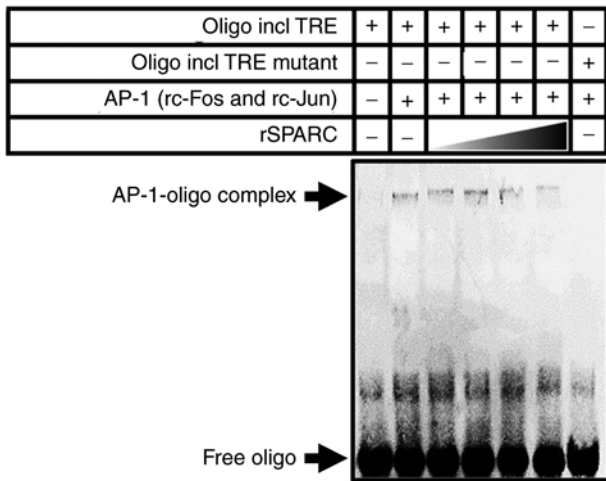


Figure 4. SPARC reduces AP-1 binding to Oligo incl TRE. Effect of SPARC on binding of AP-1 to the TRE was evaluated using an electrophoretic mobility shift assay. The recombinant AP-1 proteins (rc-Fos and/or rc-Jun) were incubated with the biotinylated Oligo incl TRE in the presence or absence of rSPARC. AP-1, activator protein-1; SPARC, secreted protein acidic and rich in cysteine; TRE, TPA-response element; Oligo incl TRE, DNA oligonucleotide containing TRE sequence; r, recombinant.

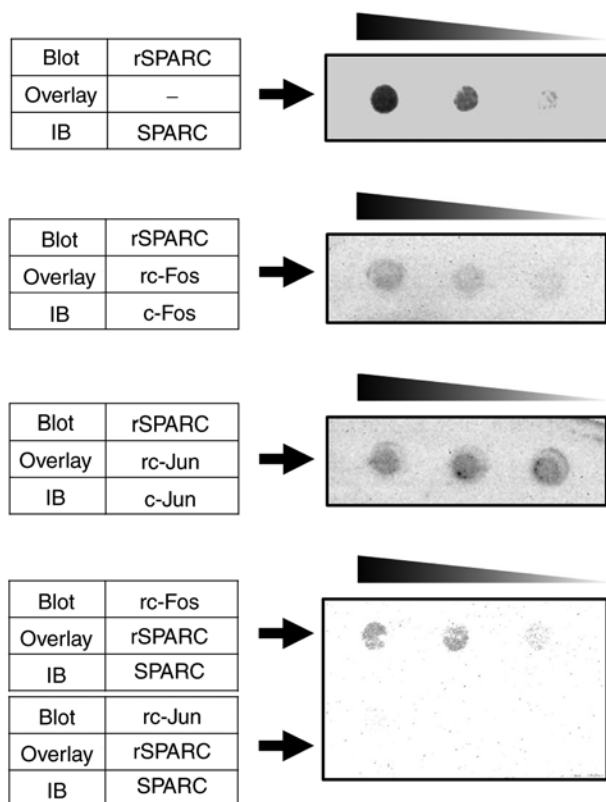


Figure 5. Binding of SPARC to c-Fos. Binding of SPARC to activator protein-1 components was evaluated using far western blotting. Briefly, the recombinant proteins were spotted on the membrane, overlaid with proteins as indicated and treated with antibodies against the overlaid proteins. The complex was visualized using the chemiluminescence method. SPARC, secreted protein acidic and rich in cysteine; r, recombinant; IB, immunoblot.

by the addition of both c-Fos and c-Jun; however, the presence of SPARC prevented those mobility shifts. Furthermore, mutation of the TRE sequence markedly abrogated complex

formation. As strong signals were not detected using the immunoprecipitation assay in preliminary experiments to assess protein-protein interaction (data not shown), far western blotting was performed to assess whether SPARC directly bound c-Fos or c-Jun to prevent the dimerization of AP-1 components. In the experiments in which the SPARC-blotting membrane was overlaid with c-Fos and the experiments in which the c-Fos-blotting membrane was overlaid with SPARC, specific and direct binding of SPARC to c-Fos was detected (Fig. 5). However, both SPARC-blotting membrane overlaid with c-Jun and c-Jun-blotting membrane overlaid with SPARC did not show any specific binding.

Discussion

The matricellular proteins include SPARC, thrombospondins, tenascins and CCNs, such as cysteine-rich 61 and connective tissue growth factor (39). Also included are members of the small integrin-binding ligand *N*-linked glycoprotein family, such as OPN, periostin, bone sialoprotein, dentin sialophosphoprotein, matrix extracellular phosphoglycoprotein and dentin matrix protein-1. These proteins function at the cell surface, interacting with cell surface receptors, growth factors, proteinases and other extracellular matrix proteins. Some of these proteins have been reported to have intracellular functions. For example, OPN has been reported to interact with the intracellular domain of CD44 (40) and thrombospondin can bind to the ER luminal domain of activating transcription factor 6 α (41). SPARC has been reported to be an intracellular protein (13-17,20); however, its function is not completely understood. The present study demonstrated that intracellular SPARC bound to c-Fos.

Phenotypically, *Sparc* KO mice have been reported to be characterized by impaired bone formation and enhanced adipose tissue formation (11). However, *c-Fos* KO mice have been reported to be characterized by osteopetrosis, a condition in which bone mass is abnormally high due to defective bone resorption; however, bone-forming activity remains unclear (42,43). As c-Fos has been reported to be activated in osteoclast precursors and to be required for osteoclast differentiation (44), Thus, c-Fos is thought to serve an important role in bone resorption through differentiation/activation of osteoclasts directly to pre-osteoclasts and/or indirectly through osteoblasts. However, to the best of our knowledge, the effects of c-Fos on adipogenesis have not been previously reported. Transgenic mice carrying Fra-1, a c-Fos-related protein and the counterpart of c-Jun, have been reported to have increased bone formation (45). Mouse adipose-derived stromal cells with higher *Fosl1* transgene expression have been reported to have reduced adipogenesis (46). *Fosl2*-transgenic mice have been reported to have an osteosclerotic phenotype due to excess osteoblastogenesis, whereas *Fosl2* KO in mice has been reported to impair osteoblastogenesis and enhance an adipogenic phenotype (47). Similarly, mice transgenic for Δ FosB have been reported to have increased osteosclerosis and reduced adipogenesis through two independent cell-autonomous mechanisms (48). Fra-1 and Fra-2 have been reported to inhibit PPAR γ expression levels, whereas c-Fos may enhance PPAR γ expression in nonalcoholic fatty liver disease (49). As Jun family members have been hypothesized to contribute

less to bone formation than Fos proteins (50), Fos proteins, with the exception of c-Fos, have been hypothesized to serve an important role in the induction of cells of the osteoblastic lineage concomitant with a decrease in adipogenesis. The phenotype of *Sparc* KO mice is highly similar to that of *Fosl2* KO mice, including low bone density and an abundance of adipose tissue (8,10,51). These findings suggested that SPARC may be involved in the activation of AP-1, via Fos proteins such as Fra-1, Fra-2 and Δ FosB. That is, SPARC may bind to c-Fos and function as a decoy counterpart of c-Fos to reduce dimerization, thus increasing the ability of other Fos proteins to dimerize with Jun, inhibiting adipogenesis and promoting osteoblastogenesis.

This hypothesis was supported by previous studies, which reported that Fra-2 suppressed PPAR γ 2 in adipocytes (51) and increased bone formation (45,52). The present study demonstrated that unstimulated basal AP-1 activity was markedly higher in SPARC-low ST2 cells compared with that in parental ST2 cells. Because most basal AP-1 activity was attributed to c-Fos, AP-1 activity may be higher in SPARC-low ST2 cells due to effects on c-Fos. That is, SPARC may inhibit the apparent basal activity of AP-1 by binding to c-Fos, suggesting that SPARC could inhibit c-Fos-containing AP-1 formation, enabling Jun proteins to dimerize with other Fos proteins, thus promoting osteoblastogenesis. The DNA-binding specificity of Fra-1/c-Jun heterodimers was previously reported to be indistinguishable from that of c-Fos/c-Jun heterodimers (53); however, a further study reported that their binding specificities were clearly distinguishable concerning PPAR γ (49). The discrepant AP-1 activity changes (AP-1 activity was higher, whereas the mRNA expression levels of the AP-1 target gene PPAR γ 2 were lower in SPARC-low ST2 cells compared with in parental ST2 cells) demonstrated in the present study may also have been due to bio-physiological conditions that limited response to the transiently introduced vector that determined promoter activity and its inability to be integrated into the genome (54).

In the present study, it was demonstrated that secreted SPARC functioned intracellularly as a decoy counterpart of c-Fos, after its incorporation from the extracellular space. The un-secreted form (absence of signal peptide) demonstrated no AP-1-inhibiting activity. Furthermore, the far western blotting assay using recombinant proteins, which were not in their glycosylated forms, demonstrated that SPARC bound c-Fos. Because SPARC is a highly glycosylated protein, it is still possible that glycosylation of SPARC may affect AP-1 activity. Further studies are required to elucidate the inhibitory mechanism.

Sparc KO mice were initially established using a Mf1/129Sv/Ev outbred mixed background by targeting exon 6 (8). Phenotypically, these mice were characterized by obvious cataract formation and adipose tissue accumulation, but their skeletal size was not changed. Other *Sparc* KO mice were established with different backgrounds and strategies. For example, 129SV/C57BL/6 *Sparc* KO mice targeting exon 4 were characterized by cataract formation, adipose tissue accumulation and osteopenia (9,10). Osteopenia was also reported in *Sparc* KO 129Sv/Ev inbred mice targeting exon 6, whereas symptoms of osteopenia were not reported in Mf1/129Sv/Ev outbred mice with *Sparc* KO because osteopenia was hidden

by high degrees of individual variability (55). Consequently, *Sparc* deficiency has been reported to exert skeletal effects that are not as severe as adipose tissue accumulation (9). Notably, the ability of SPARC to inhibit adipogenesis was not hidden by high degrees of individual variability, which suggested that SPARC strongly inhibited adipogenesis but did not strongly induce osteoblastogenesis. This inhibition of adipogenesis suggested that SPARC was involved in the commitment of bone marrow stromal cells to differentiation into osteoblasts.

SPARC levels (both mRNA and protein) have been reported to be closely related to obesity and diabetes mellitus. Weight loss resulting from a very low-calorie diet has been reported to cause a concomitant 33% reduction of *SPARC* gene expression in adipose tissue, whereas weight gain through consumption of a fast-food diet increased *SPARC* gene expression in adipose tissue by 30% (56). SPARC expression has also been reported to be correlated with leptin-independent fat mass and insulin resistance (56), associations supported by the high SPARC expression in adipose tissue of leptin receptor-deficient mice (57). *SPARC* mRNA expression levels in both abdominal and visceral adipose tissue have been reported to be correlated with body mass index, and serum SPARC concentration has been shown to be associated with fasting insulin concentration and the homeostasis model assessment of insulin resistance score (58).

The aforementioned clinical observations seemingly oppose the *Sparc* KO phenotype being the accumulation of adipose tissue; however, SPARC no doubt serves an important role in the regulation of adipogenesis, as well as in bone marrow stromal cell differentiation, committing cells to the osteoblast lineage through inhibition of adipogenesis as a decoy counterpart of c-Fos. Our findings suggest providing novel insights into regenerative medicine.

Acknowledgements

The present study was based on a PhD thesis (Tomoya Hatori), which was published by Ohu University Press in 2020.

Funding

The present study was supported by JSPS KAKENHI (grant nos. JP17K11885, JP18K09642 and JP19K10074).

Availability of data and materials

The datasets used and/or analyzed during the current study are available from the corresponding author on reasonable request.

Authors' contributions

TH and YK wrote the manuscript. TH, TM and AS performed the experiments. TH, KT and YK analyzed the data. TM, KT and YK designed the experiments. TH, TM and YK confirm the authenticity of all the raw data. All authors read and approved the final manuscript.

Ethics approval and consent to participate

Not applicable.

Patient consent for publication

Not applicable.

Competing interests

The authors declare that they have no competing interests.

References

- Termine JD, Kleinman HK, Whitson SW, Conn KM, McGarvey ML and Martin GR: Osteonectin, a bone-specific protein linking mineral to collagen. *Cell* 26: 99-105, 1981.
- Yan Q and Sage EH: SPARC, a matricellular glycoprotein with important biological functions. *J Histochem Cytochem* 47: 1495-1506, 1999.
- Bradshaw AD: The role of SPARC in extracellular matrix assembly. *J Cell Commun Signal* 3: 239-246, 2009.
- Murphy-Ullrich JE and Sage EH: Revisiting the matricellular concept. *Matrix Biol* 37: 1-14, 2014.
- Giudici C, Raynal N, Wiedemann H, Cabral WA, Marini JC, Timpl R, Bächinger HP, Farndale RW, Sasaki T and Tenni R: Mapping of SPARC/BM-40/osteonectin-binding sites on fibrillar collagens. *J Biol Chem* 283: 19551-19560, 2008.
- Duncan S, Delage S, Chioran A, Sirbu O, Brown TJ and Ringuette MJ: The predicted collagen-binding domains of Drosophila SPARC are essential for survival and for collagen IV distribution and assembly into basement membranes. *Dev Biol* 461: 197-209, 2020.
- Cydzik M, Abdul-Wahid A, Park S, Bourdeau A, Bowden K, Prodeus A, Kollara A, Brown TJ, Ringuette MJ and Gariépy J: Slow binding kinetics of secreted protein, acidic, rich in cysteine-VEGF interaction limit VEGF activation of VEGF receptor 2 and attenuate angiogenesis. *FASEB J* 29: 3493-3505, 2015.
- Gilmour DT, Lyon GJ, Carlton MB, Sanes JR, Cunningham JM, Anderson JR, Hogan BL, Evans MJ and Colledge WH: Mice deficient for the secreted glycoprotein SPARC/osteonectin/BM40 develop normally but show severe age-onset cataract formation and disruption of the lens. *EMBO J* 17: 1860-1870, 1998.
- Delany AM, Amling M, Priemel M, Howe C, Baron R and Canalis E: Osteopenia and decreased bone formation in osteonectin-deficient mice. *J Clin Invest* 105: 915-923, 2000.
- Bradshaw AD, Graves DC, Motamed K and Sage EH: SPARC-null mice exhibit increased adiposity without significant differences in overall body weight. *Proc Natl Acad Sci USA* 100: 6045-6050, 2003.
- Delany AM, Kalajzic I, Bradshaw AD, Sage EH and Canalis E: Osteonectin-null mutation compromises osteoblast formation, maturation, and survival. *Endocrinology* 144: 2588-2596, 2003.
- Francki A, Bradshaw AD, Bassuk JA, Howe CC, Couser WG and Sage EH: SPARC regulates the expression of collagen type I and transforming growth factor-beta1 in mesangial cells. *J Biol Chem* 274: 32145-32152, 1999.
- Yan Q, Weaver M, Perdue N and Sage EH: Matricellular protein SPARC is translocated to the nuclei of immortalized murine lens epithelial cells. *J Cell Physiol* 203: 286-294, 2005.
- Gooden MD, Vernon RB, Bassuk JA and Sage EH: Cell cycle-dependent nuclear location of the matricellular protein SPARC: Association with the nuclear matrix. *J Cell Biochem* 74: 152-167, 1999.
- Hecht JT and Sage EH: Retention of the matricellular protein SPARC in the endoplasmic reticulum of chondrocytes from patients with pseudoachondroplasia. *J Histochem Cytochem* 54: 269-274, 2006.
- Huynh MH, Hong H, Delovitch S, Desser S and Ringuette M: Association of SPARC (osteonectin, BM-40) with extracellular and intracellular components of the ciliated surface ectoderm of *Xenopus* embryos. *Cell Motil Cytoskeleton* 47: 154-162, 2000.
- Sodek J, Zhu B, Huynh MH, Brown TJ and Ringuette M: Novel functions of the matricellular proteins osteopontin and osteonectin/SPARC. *Connect Tissue Res* 43: 308-319, 2002.
- Krstulja M, Car A, Bonifacić D, Braut T and Kujundzić M: Nasopharyngeal angiofibroma with intracellular accumulation of SPARC—a hypothesis (SPARC in nasopharyngeal angiofibroma). *Med Hypotheses* 70: 600-604, 2008.
- Fenouille N, Puissant A, Dufies M, Robert G, Jacquet A, Ohanna M, Deckert M, Pasquet JM, Mahon FX, Cassuto JP, *et al*: Persistent activation of the Fyn/ERK kinase signaling axis mediates imatinib resistance in chronic myelogenous leukemia cells through upregulation of intracellular SPARC. *Cancer Res* 70: 9659-9670, 2010.
- Vinayagam A, Stelzl U, Foulle R, Plassmann S, Zenkner M, Timm J, Assmus HE, Andrade-Navarro MA and Wanker EE: A directed protein interaction network for investigating intracellular signal transduction. *Sci Signal* 4: rs8, 2011.
- White UA and Stephens JM: Transcriptional factors that promote formation of white adipose tissue. *Mol Cell Endocrinol* 318: 10-14, 2010.
- Karin M, Liu ZG and Zandi E: AP-1 function and regulation. *Curr Opin Cell Biol* 9: 240-246, 1997.
- Distel RJ, Ro HS, Rosen BS, Groves DL and Spiegelman BM: Nucleoprotein complexes that regulate gene expression in adipocyte differentiation: Direct participation of c-fos. *Cell* 49: 835-844, 1987.
- Knebel B, Kotzka J, Lehr S, Hartwig S, Avci H, Jacob S, Nitzgen U, Schiller M, März W, Hoffmann MM, *et al*: A mutation in the c-fos gene associated with congenital generalized lipodystrophy. *Orphanet J Rare Dis* 8: 119, 2013.
- Maeda T and Horiuchi N: Simvastatin suppresses leptin expression in 3T3-L1 adipocytes via activation of the cyclic AMP-PKA pathway induced by inhibition of protein prenylation. *J Biochem* 145: 771-781, 2009.
- Maeda T, Suzuki A, Yuzawa S, Baba Y, Kimura Y and Kato Y: Mineral trioxide aggregate induces osteoblastogenesis via Atf6. *Bone Rep* 2: 36-43, 2015.
- Hirose K, Isogai E, Mizugai H and Ueda I: Adhesion of *Porphyromonas gingivalis* fimbriae to human gingival cell line Ca9-22. *Oral Microbiol Immunol* 11: 402-406, 1996.
- Ogawa M, Nishikawa S, Ikuta K, Yamamura F, Naito M, Takahashi K and Nishikawa S: B cell ontogeny in murine embryo studied by a culture system with the monolayer of a stromal cell clone, ST2: B cell progenitor develops first in the embryonal body rather than in the yolk sac. *EMBO J* 7: 1337-1343, 1988.
- Chomczynski P and Sacchi N: Single-step method of RNA isolation by acid guanidinium thiocyanate-phenol-chloroform extraction. *Anal Biochem* 162: 156-159, 1987.
- Schmittgen TD and Livak KJ: Analyzing real-time PCR data by the comparative C(T) method. *Nat Protoc* 3: 1101-1108, 2008.
- Nagaoka M, Maeda T, Chatani M, Handa K, Yamakawa T, Kiyohara S, Negishi-Koga T, Kato Y, Takami M, Niida S, *et al*: A delphinidin-enriched maqui berry extract improves bone metabolism and protects against bone loss in osteopenic mouse models. *Antioxidants (Basel)* 8: 386, 2019.
- Dignam JD, Lebovitz RM and Roeder RG: Accurate transcription initiation by RNA polymerase II in a soluble extract from isolated mammalian nuclei. *Nucleic Acids Res* 11: 1475-1489, 1983.
- Maeda T, Suzuki A, Koga K, Miyamoto C, Maehata Y, Ozawa S, Hata RI, Nagashima Y, Nabeshima K, Miyazaki K and Kato Y: TRPM5 mediates acidic extracellular pH signaling and TRPM5 inhibition reduces spontaneous metastasis in mouse B16-BL6 melanoma cells. *Oncotarget* 8: 78312-78326, 2017.
- Hellman LM and Fried MG: Electrophoretic mobility shift assay (EMSA) for detecting protein-nucleic acid interactions. *Nat Protoc* 2: 1849-1861, 2007.
- Cornelius P, MacDougald OA and Lane MD: Regulation of adipocyte development. *Annu Rev Nutr* 14: 99-129, 1994.
- Maeda T, Kawane T and Horiuchi N: Statins augment vascular endothelial growth factor expression in osteoblastic cells via inhibition of protein prenylation. *Endocrinology* 144: 681-692, 2003.
- Garin-Shkolnik T, Rudich A, Hotamisligil GS and Rubinstein M: FABP4 attenuates PPAR γ and adipogenesis and is inversely correlated with PPAR γ in adipose tissues. *Diabetes* 63: 900-911, 2014.
- Tseng C and Kolonin MG: Proteolytic isoforms of SPARC induce adipose stromal cell mobilization in obesity. *Stem Cells* 34: 174-190, 2016.
- Kawakita F, Kanamaru H, Asada R and Suzuki H: Potential roles of matricellular proteins in stroke. *Exp Neurol* 322: 113057, 2019.
- Suzuki K, Zhu B, Rittling SR, Denhardt DT, Goldberg HA, McCulloch CA and Sodek J: Colocalization of intracellular osteopontin with CD44 is associated with migration, cell fusion, and resorption in osteoclasts. *J Bone Miner Res* 17: 1486-1497, 2002.

41. Lynch JM, Mailliet M, Vanhoutte D, Schloemer A, Sargent MA, Blair NS, Lynch KA, Okada T, Aronow BJ, Osinska H, *et al*: A thrombospondin-dependent pathway for a protective ER stress response. *Cell* 149: 1257-1268, 2012.
42. Grigoriadis AE, Wang ZQ, Cecchini MG, Hofstetter W, Felix R, Fleisch HA and Wagner EF: c-Fos: A key regulator of osteoclast-macrophage lineage determination and bone remodeling. *Science* 266: 443-448, 1994.
43. Wang ZQ, Ovitt C, Grigoriadis AE, Möhle-Steinlein U, Rütter U and Wagner EF: Bone and haematopoietic defects in mice lacking c-fos. *Nature* 360: 741-745, 1992.
44. Boyce BF, Yamashita T, Yao Z, Zhang Q, Li F and Xing L: Roles for NF-kappaB and c-Fos in osteoclasts. *J Bone Miner Metab* 23 (Suppl 1): S11-S15, 2005.
45. Jochum W, David JP, Elliott C, Wutz A, Plenk H Jr, Matsuo K and Wagner EF: Increased bone formation and osteosclerosis in mice overexpressing the transcription factor Fra-1. *Nat Med* 6: 980-984, 2000.
46. Schwabe K, Garcia M, Ubieta K, Hannemann N, Herbolt B, Luther J, Noël D, Jorgensen C, Casteilla L, David JP, *et al*: Inhibition of osteoarthritis by adipose-derived stromal cells overexpressing Fra-1 in mice. *Arthritis Rheumatol* 68: 138-151, 2016.
47. Eferl R, Hasselblatt P, Rath M, Popper H, Zenz R, Komnenovic V, Idarraga MH, Kenner L and Wagner EF: Development of pulmonary fibrosis through a pathway involving the transcription factor Fra-2/AP-1. *Proc Natl Acad Sci USA* 105: 10525-10530, 2008.
48. Kveiborg M, Sabatakos G, Chiusaroli R, Wu M, Philbrick WM, Horne WC and Baron R: DeltaFosB induces osteosclerosis and decreases adipogenesis by two independent cell-autonomous mechanisms. *Mol Cell Biol* 24: 2820-2830, 2004.
49. Hasenfuss SC, Bakiri L, Thomsen MK, Williams EG, Auwerx J and Wagner EF: Regulation of steatohepatitis and PPAR γ signaling by distinct AP-1 dimers. *Cell Metab* 19: 84-95, 2014.
50. Wagner EF and Eferl R: Fos/AP-1 proteins in bone and the immune system. *Immunol Rev* 208: 126-140, 2005.
51. Luther J, Ubieta K, Hannemann N, Jimenez M, Garcia M, Zech C, Schett G, Wagner EF and Bozec A: Fra-2/AP-1 controls adipocyte differentiation and survival by regulating PPAR γ and hypoxia. *Cell Death Differ* 21: 655-664, 2014.
52. Roschger P, Matsuo K, Misof BM, Tesch W, Jochum W, Wagner EF, Fratzl P and Klaushofer K: Normal mineralization and nanostructure of sclerotic bone in mice overexpressing Fra-1. *Bone* 34: 776-782, 2004.
53. Cohen DR, Ferreira PC, Gentz R, Franza BR Jr and Curran T: The product of a fos-related gene, fra-1, binds cooperatively to the AP-1 site with Jun: Transcription factor AP-1 is comprised of multiple protein complexes. *Genes Dev* 3: 173-184, 1989.
54. Yan C, Wang H, Aggarwal B and Boyd DD: A novel homologous recombination system to study 92 kDa type IV collagenase transcription demonstrates that the NF-kappaB motif drives the transition from a repressed to an activated state of gene expression. *FASEB J* 18: 540-541, 2004.
55. Mansergh FC, Wells T, Elford C, Evans SL, Perry MJ, Evans MJ and Evans BA: Osteopenia in Sparc (osteonectin)-deficient mice: Characterization of phenotypic determinants of femoral strength and changes in gene expression. *Physiol Genomics* 32: 64-73, 2007.
56. Kos K, Wong S, Tan B, Gummesson A, Jernas M, Franck N, Kerrigan D, Nystrom FH, Carlsson LM, Randeve HS, *et al*: Regulation of the fibrosis and angiogenesis promoter SPARC/osteonectin in human adipose tissue by weight change, leptin, insulin, and glucose. *Diabetes* 58: 1780-1788, 2009.
57. Tartare-Deckert S, Chavey C, Monthouel MN, Gautier N and Van Obberghen E: The matricellular protein SPARC/osteonectin as a newly identified factor up-regulated in obesity. *J Biol Chem* 276: 22231-22237, 2001.
58. Lee SH, Lee JA, Park HS, Song YS, Jang YJ, Kim JH, Lee YJ and Heo Y: Associations among SPARC mRNA expression in adipose tissue, serum SPARC concentration and metabolic parameters in Korean women. *Obesity (Silver Spring)* 21: 2296-2302, 2013.



This work is licensed under a Creative Commons Attribution-NonCommercial-NoDerivatives 4.0 International (CC BY-NC-ND 4.0) License.